Articles

Competitive Antagonism of AMPA Receptors by Ligands of Different Classes: Crystal Structure of ATPO Bound to the GluR2 Ligand-Binding Core, in Comparison with DNQX

Anders Hogner,[†] Jeremy R. Greenwood,[†] Tommy Liljefors,[†] Marie-Louise Lunn,[†] Jan Egebjerg,[‡]
Ingrid K. Larsen,[†] Eric Gouaux,[§,▽] and Jette S. Kastrup*,[†]

*Department of Medicinal Chemistry, Royal Danish School of Pharmacy, Universitetsparken 2, DK 2100 Copenhagen, Denmark,
Department for Molecular and Structural Biology, University of Aarhus, DK-8000 Aarhus, Denmark, Department of
Biochemistry and Molecular Biophysics, Columbia University, 650 W. 168th Street, New York, New York 10032, and Howard
Hughes Medical Institute, Columbia University, New York, New York 10032*

Received July 10, 2002

Ionotropic glutamate receptors (iGluRs) constitute a family of ligand-gated ion channels that are essential for mediating fast synaptic transmission in the central nervous system. This study presents a high-resolution X-ray structure of the competitive antagonist (*S*)-2-amino-3-[5-*tert*-butyl-3-(phosphonomethoxy)-4-isoxazolyl]propionic acid (ATPO) in complex with the ligand-binding core of the receptor. Comparison with the only previous structure of the ligand-binding core in complex with an antagonist, 6,7-dinitro-2,3-quinoxalinedione (DNQX) (Armstrong, N.; Gouaux, E. *Neuron* **2000**, *28*, 165−181), reveals that ATPO and DNQX stabilize an open form of the ligand-binding core by different sets of interactions. Computational techniques are used to quantify the differences between these two ligands and to map the binding site. The isoxazole moiety of ATPO acts primarily as a spacer, and other scaffolds could potentially be used. Whereas agonists induce substantial domain closures compared to the *apo* structure, ATPO only induces minor conformational changes. These results are consistent with the hypothesis that domain closure is related to receptor activation. To facilitate the design of novel AMPA receptor antagonists, we present a modified model of the binding site that includes key residues involved in ligand recognition.

Introduction

(*S*)-Glutamic acid (Glu) is the major excitatory neurotransmitter in the central nervous system (CNS). Glutamate operates via ligand-gated ion channels (iGluRs) and G-protein-coupled metabotropic receptors (mGluRs).[1] The iGluRs play a central role in rapid neural signaling and in regulation of synaptic strength, but are also implicated in a number of serious psychiatric and neurological diseases.[1,2] The iGluRs are divided into three classes based on their affinities and functional responses to the agonists 2-amino-3-(3-hydroxy-5-methyl-4-isoxazolyl)propionic acid (AMPA), kainic acid (KA), and *N*-methyl-D-aspartic acid (NMDA).[3] These membrane-bound receptors are assembled from class-specific combinations of homo- or heteromeric subunits. AMPA receptors are formed from the subunits GluR1-4.[4] Combinations of GluR5-7 and KA1-2 form the KA receptors, and the subunits NR1, NR2A-2D, and NR3A-B assemble to form NMDA receptors.[1,3] Recent

evidence suggests that these receptors are tetramers, assembled as dimers-of-dimers.[5−10] The variety of subunit combinations, the expression of either the flip(i) or the flop(o) splice variants,[11] and post-transcriptional RNA editing result in a broad diversity of iGluRs.[12] This heterogeneity is reflected in the observed pharmacological and functional properties.[1,13] The topology of a single iGluR subunit is defined by (1) an amino terminal domain (ATD); (2) a ligand binding core (S1 and S2); (3) three membrane spanning regions (M1, M2, and M3) plus a cytoplasm-facing re-entrant loop (P); and (4) a short C-terminal intracellular region (Figure 1a).[14−16]

The structural details of ligand-binding to iGluRs were unknown until recently. A breakthrough occurred with the X-ray structure of KA bound to the ligand-binding core (S1S2) of the AMPA receptor subunit GluR2o.[17] This achievement was facilitated by the finding that the transmembrane regions M1 and M2 could be substituted by a peptide linker, and that the ATD and the last transmembrane segment could be deleted. The resulting soluble fusion proteins displayed binding affinities that were comparable with that of the full-length membrane-bound receptor.[15,18] The development of facile expression and purification methodologies for GluR2-S1S2 constructs has enabled the determination of the crystal structures of six agonists and of the
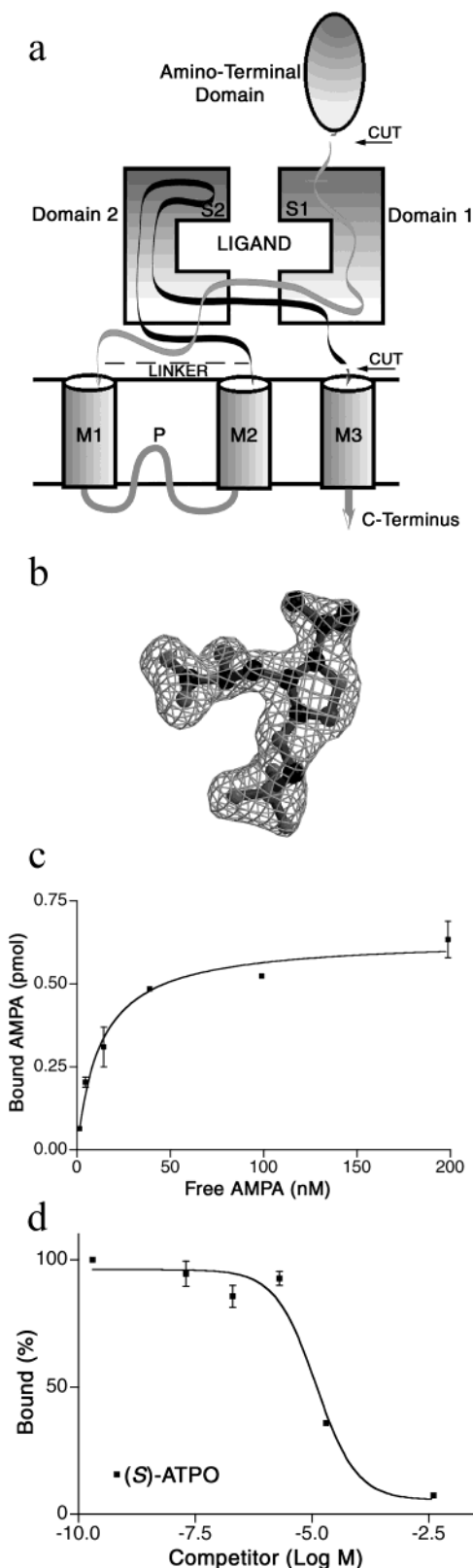
* To whom correspondence should be addressed: Tel: +4535306486, Fax: +4535306040, E-mail: jsk@dfh.dk.
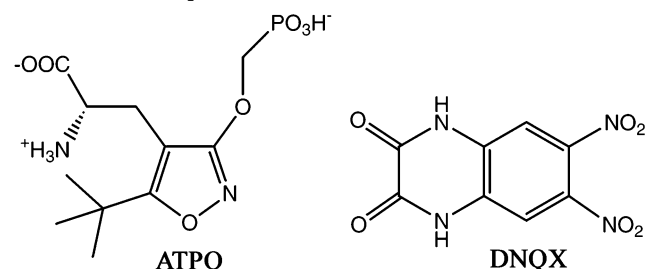 † Royal Danish School of Pharmacy.
  ‡ University of Aarhus.
  § Department of Biochemistry and Molecular Biophysics, Columbia University.
  ▽ Howard Hughes Medical Institute, Columbia University.

Chart 1. Two Competitive AMPA Receptor Antagonists.
ATPO: (*S*)-2-Amino-3-[5-*tert*-butyl-3-(phosphono-
methoxy)-4-isoxazolyl]propionic Acid. DNQX:
6,7-Dinitro-2,3-quinoxalinedione

antagonist 6,7-dinitro-2,3-quinoxalinedione (DNQX, see
Chart 1) in complex with GluR2-S1S2, as well as the
apo structure.[5,19] The structures have revealed different
degrees of closure of the cleft between the two domains
forming the bilobular structure. Full agonists such as
Glu and AMPA induce 20° of domain closure compared
to the *apo* structure, whereas the antagonist DNQX
stabilizes an open conformation.

A large number of iGluR antagonists have been
synthesized and characterized pharmacologically.[1,20]
Over the years, these have incrementally advanced our
understanding of the structural characteristics involved
in the antagonism of iGluRs. However, to our knowl-
edge, no competitive antagonist has yet been shown to
exhibit significant subtype selectivity between ho-
momers of the four AMPA-sensitive subunits (GluR1-
4). Even though the GluR2-S1S2:DNQX structure pro-
vided a significantly better understanding of the
fundamental details of antagonist binding, many ques-
tions remain unanswered. For example, will other
antagonists stabilize the same open conformation of
S1S2 as DNQX? Do structurally dissimilar antagonists
share the same binding mode? Which structural fea-
tures are important for the design of a subunit selective,
high affinity antagonist? To address such questions, we
have determined the high-resolution X-ray structure of
the competitive AMPA receptor antagonist (*S*)-2-amino-
3-[5-*tert*-butyl-3-(phosphonomethoxy)-4-isoxazolyl]pro-
pionic acid (ATPO)[21,22] (see Chart 1) in complex with
GluR2-S1S2. Moreover, detailed analyses of both the
ligands and of the binding site using computational
techniques have been undertaken.

Results and Discussion

The high-resolution X-ray structure of the GluR2
ligand-binding core S1S2J in complex with (*S*)-ATPO
was solved at 2.1 Å resolution, as documented in Table
1 and Figure 1b. There are four protein molecules in
the asymmetric unit (a.u.) of the unit cell (designated
ATPO:A−D). Pairwise superimposition of the Cα-atoms
of the four molecules yields root-mean square deviations
(rmsd) of 0.4−0.8 Å. To verify that S1S2J behaves in a
similar way to full-length AMPA receptors, the K_D value
for [³H]AMPA and the IC_{50} value for displacement by
(*S*)-ATPO were determined. The binding affinity for
AMPA and the IC_{50} value for ATPO (Figure 1c,d) were
found to be in good agreement with AMPA receptor
pharmacology on full-length receptors (K_D for [³H]AMPA
binding is 12 nM and IC_{50} of ATPO is 16 μM).[22,23]

Binding Interactions between ATPO and S1S2J.
ATPO binds within the open cleft between domain 1 and

Figure 1. Schematic representation of the iGluR subunit
topology, omit electron density map of ATPO, and ligand-
binding pharmacology. (a) The topology of an iGluR subunit.
The two segments S1 (in gray) and S2 (in black) form the
bilobular structure of the ligand-binding core. Cut and linker
denote the boundaries for the GluR2-S1S2J construct. (b) F_o
− F_c omit electron density map contoured at 3.0σ for S1S2J:
ATPO (protomer A). (c) K_D for [³H]AMPA binding is 12.8 ±
1.9 nM. (d) IC_{50} for displacement of [³H]-AMPA by (*S*)-ATPO
on GluR2-S1S2J is 12.2 μM.

Table 1. Data Collection and Refinement Statistics for GluR2-S1S2J:ATPO

|	
space group	$P2_12_12_1$
unit cell (Å)	$a = 66.0$
	$b = 89.1$
	$c = 194.9$
no. per a.u.[a]	4
crystal mosaicity (deg)	0.6
resol. (Å)	20−2.10
total obs	490208
unique obs	66583
$I/\sigma(I)$[b]	20.2 (3.4)
completeness (%)[b]	99.1 (98.6)
R_{merge} (%)[b,c]	9.8 (59.5)
R_{work} (%)[d]	19.4
R_{free} (%)[e]	24.5
no. protein/ligand/water atoms	8040/84/949
no. acetate/sulfate ions	1/4
average B-values (Å^2)	29.4
rms bond lengths (Å)	0.005
rms bond angles (deg)	1.2
residues in allowed regions (%)[f]	99.7

[a] Number of protein molecules per asymmetric unit (a.u). [b] Values in parentheses are statistics for the highest resolution bin (2.17−2.10 Å). [c] R_{merge} (I) = $\Sigma_{hkl} |I_{hkl} - \langle I_{hkl}\rangle|/\Sigma_{hkl} I_{hkl}$, where I_{hkl} is the measured intensity of the reflections with indices hkl. [d] $R_{work} = \Sigma_{hkl} ||F_o| - |F_c||/\Sigma|F_o|$, where $|F_o|$ and $|F_c|$ are the observed and calculated structure factor amplitudes for reflection hkl, respectively. [e] Five percent of the reflections in the data set were set aside for calculation of the R_{free} value. [f] The Ramachandran plot was calculated according to Kleywegt et al.[44]

domain 2. The α-carboxylate and the α-ammonium groups of ATPO interact through hydrogen bonds and ion-pair interactions with the conserved amino acids Pro478, Thr480, and Arg485 from domain 1 and Glu705 from domain 2 (Figure 2a). These also are key residues for binding the corresponding groups of agonists,[5,19] although the isoxazole moieties of ATPO and AMPA interact differently with the receptor. Superimposition of the ATPO and DNQX complexes clearly shows how the two structurally dissimilar antagonists obtain comparable binding interactions with these conserved residues (Figure 3). The α-carboxylate and the α-ammonium groups of ATPO overlay well with the two carbonyl groups and one of the amide nitrogens of the quinoxalinedione ring of DNQX. The isoxazole ring of ATPO forms only a single, indirect interaction with the protein, from the nitrogen atom via a water molecule W2 to Glu705 (Table 2 and Figure 2a).

The phosphonate group of ATPO is involved in an extensive hydrogen bonding network, interacting directly with Ser654, Thr655, and Glu705, and forming indirect contacts with the protein through six water molecules (Figure 2a and Table 2). Residues Ser654, Thr655, and Glu705 are also important for agonist binding.[5,19] The side-chain OE2 atom of Glu705 forms hydrogen bonds to both the α-ammonium group of ATPO and to the oxygen O4 of the phosphonate group, implying that O4 is protonated. In the S1S2J:DNQX complex a sulfate ion was modeled into the electron density in one of the protomers.[5] The phosphonate group of ATPO appears at the same position as the sulfate ion (Figure 3), as previously suggested by Armstrong and Gouaux.[5] This indicates that the protein environment in this region is favorable for accommodating a large negatively charged group. The bulky *tert*-butyl group at the 5-position of the isoxazole ring is partly buried in a pocket formed by residues Glu402, Tyr405,
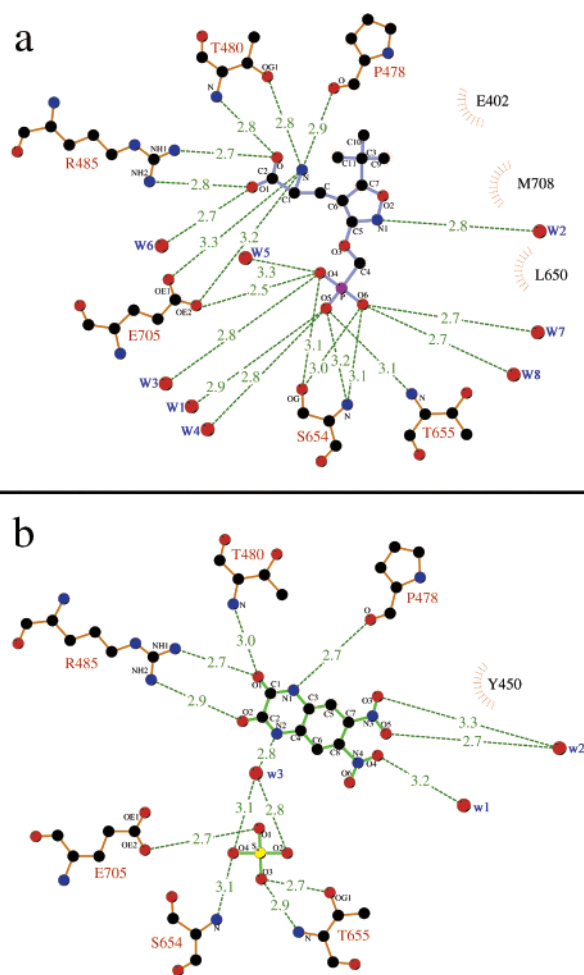
Figure 2. Schematic drawings showing the interactions of the two antagonists ATPO and DNQX with the GluR2-S1S2J protein. (a) S1S2J:ATPO (protomer A) and (b) S1S2J:DNQX (protomer B). The bonds of the antagonists and of the protein are displayed in blue and yellow, respectively. Water molecules are shown as red spheres, indicated by W and w for ATPO and DNQX complexes, respectively. Remaining atoms are in standard atomic colors (carbon is black, oxygen is red, nitrogen is blue, sulfur is yellow, and phosphorus is purple). Dashed green lines indicate all potential hydrogen bonds or ionic interactions within 3.3 Å. 'Radiating' spheres indicate hydrophobic contacts within 3.9 Å between carbon atoms in the antagonist and neighboring residues. This figure was prepared with the program Ligplot.[45]

and Tyr450 of domain 1 and Glu705, Thr707, Met708, and Tyr732 of domain 2.

Analysis of the Ligands and their Interactions. ATPO and DNQX have been investigated with the aim of gaining a better understanding of which factors play a role in determining AMPA receptor antagonist affinity. ATPO and DNQX are tri-ionized and neutral, respectively, in water at physiological pH,[24,25] and our analysis suggests that these forms are also present in the polar binding site. ATPO is a comparatively weak AMPA antagonist; the IC$_{50}$ of DNQX is 1 μM[5] while it is 12.2 μM for ATPO, i.e. ca. 12 times weaker in [^{3}H]-AMPA displacement experiments. Interestingly, some DNQX analogues show low-nanomolar affinity.[26] These compounds are generally highly insoluble in water, which has led to their abandonment in clinical trials. Even though no ATPO analogues have shown such high
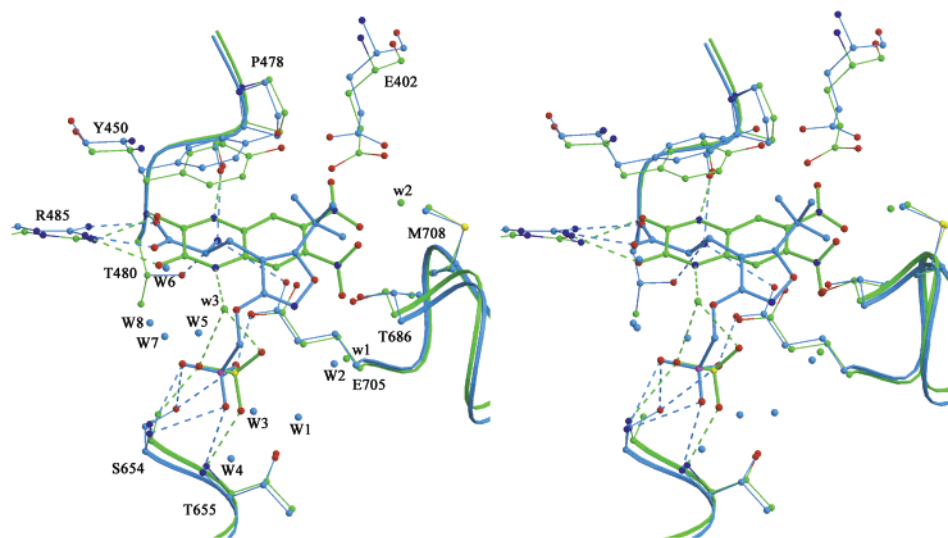
Figure 3. Stereoplot illustrating the binding modes of ATPO and DNQX in GluR2-S1S2J. The structure of S1S2J:ATPO was superimposed onto the structure of S1S2J:DNQX, using protomers A and B, respectively. Superpositions are on all Cα atoms. Backbone, selected side chains, and ligands are blue and green for the ATPO and DNQX complexes, respectively. Oxygen atoms are red, nitrogen atoms are blue, sulfur is yellow, and phosphorus is purple. Water molecules corresponding to the structures of S1S2J:ATPO and S1S2J:DNQX are shown as blue and green spheres, respectively. Dashed lines, blue between ATPO and S1S2J and green between DNQX and S1S2J, indicate all direct hydrogen bonds between ligand and the protein, as well as bonds to the sulfate ion in the DNQX complex. The figure was prepared with the programs MOLSCRIPT[46] and Raster3D.[47]

Table 2. Amino Acid Residues in GluR2-S1S2J:ATPO Involved in Water-Mediated Hydrogen Bonds to the Antagonist

water	residue	atom name	hydrogen bonding distances[a]			
			A	B	C	D
W1	Thr655	OG1	2.9	2.5	2.5	2.6
W2	Glu705	N	3.0	2.9	3.0	2.8
W3	Lys218	NZ	2.4	2.8	2.6	2.7
W3	Ser654	OG	–	2.7	2.9	3.0
W3	Thr655	OG1	2.9	–	2.7	2.9
W3	Thr655	N	–	3.1	–	–
W4	Ser652	O	2.9	–	3.1	3.0
W4	Thr655	N	–	–	3.2	–
W4	Lys656	N	3.2	–	2.6	2.9
W5	Thr480	OG1	2.5	–	–	–
W5	Glu705	OE2	2.6	–	–	–

a Potential hydrogen bonds within 3.2 Å are listed. A–D refers to the four molecules of the a.u. of the crystal.

affinity, this series may be of clinical interest on account of high aqueous solubility.

The total free energy of binding of a ligand to a protein may be divided into several discrete components: The ligand–protein interaction energy, the energy of solvation-desolvation, and the conformational energy penalty for binding. Our studies show that ATPO and DNQX vary substantially in each of these components.

Considering the strength of interaction between the ligand and the receptor, we note that ATPO and DNQX bind with strikingly different hydrogen bonding networks (Figure 2). Where ATPO is involved in ca. 21 hydrogen bonds, DNQX has only eight. Among these polar contacts, ATPO forms two strong ion-pair interactions and an ion–dipole interaction, whereas DNQX has just one ion–dipole interaction (Arg485–dione). It is clear that the hydrogen bonding interaction between ATPO and the receptor is much stronger than that of DNQX. Both ligands have van der Waals interactions with the receptor, though DNQX is further stabilized by π-stacking interactions between the aromatic ring of Tyr450 and the quinoxalinedione ring system.

Offsetting this difference in interaction energy, the two ligands have significantly different desolvation energies; ATPO is much more strongly solvated in aqueous solution than DNQX. We calculated the free energies of solvation as being ca. −88 and −31 kcal/mol for ATPO and DNQX, respectively, a difference substantially larger than the observed difference in binding (see computational methods). This large difference must be almost completely canceled by the interaction energies.

The conformational energy penalty can be divided into entropic and enthalpic terms. ATPO is a highly flexible ligand whereas DNQX is essentially rigid with little or no conformational energy penalty. Conformational analysis of ATPO is confounded by strong intramolecular hydrogen bonding for the highly charged ligand and is difficult to determine accurately. We performed a Monte Carlo conformational analysis on ATPO and found that the global minimum in water resembles the binding mode in the X-ray structure closely (rmsd heavy atoms 0.8 Å), apart from the formation of an intramolecular hydrogen bond between the α-ammonium and phosphonate groups; the cost of breaking this bond to reach the side-chain conformation corresponding to the binding mode was calculated to be 5.4 kcal/mol. As an aside, including explicit water or butyrate (modeling Glu705) in the Monte Carlo search facilitates breaking the intramolecular hydrogen bond and returns the binding mode as a low-energy minimum. In terms of entropy, the ensemble for ATPO was found to have a large number of low-energy conformations, with four rotatable bonds determining the overall conformation, at a typical cost of 0.5 kcal/mol per bond.[27]

To summarize, ATPO has a strong interaction with the receptor, a large penalty of desolvation, and a modest conformational energy penalty. DNQX has a relatively weak interaction with the receptor, a lesser desolvation energy, and minimal conformational energy penalty. From a design perspective, conformational
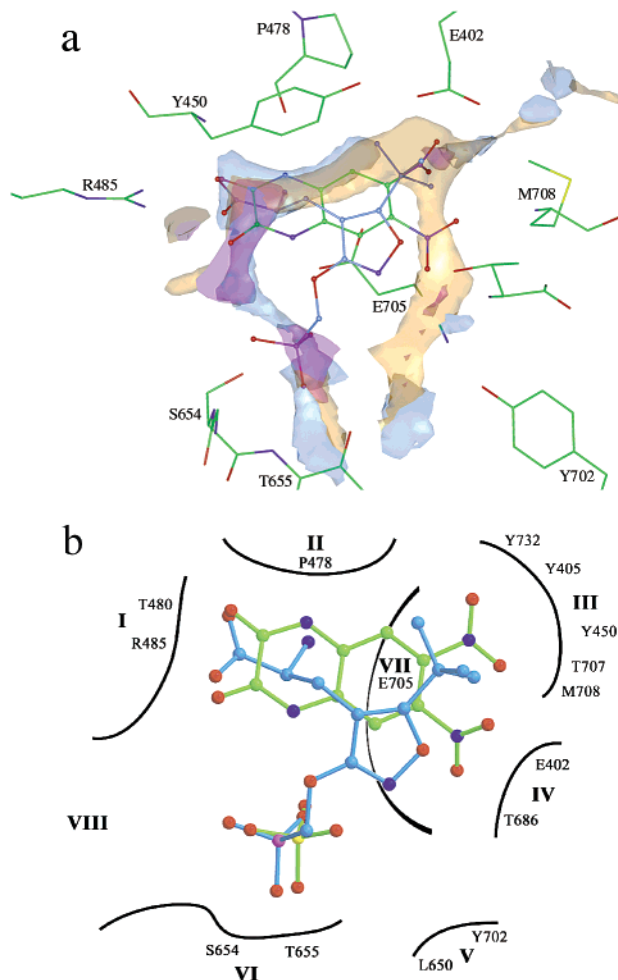
Figure 4. (a) Overlaid grid maps of the GluR2-S1S2J binding site cavity. Isoenergy contours are depicted for the methyl probe (beige, −2.9 kcal/mol), water probe (cyan, −8.5 kcal/mol), and hydrogen phosphate anion probe (violet, −14.4 kcal/mol). Selected residues are shown for the ATPO complex. (b) Schematic representation of the antagonist binding cleft of S1S2J with the two antagonists ATPO and DNQX overlaid. Sites I to VIII, including key residues, indicate regions, which may be important for the design of new selective antagonists. In a and b, ATPO and DNQX are shown in blue and green, respectively, with the same coloring scheme for the atoms as in Figure 3.

restriction and greater hydrophobic contact would be desirable for increasing the affinity of ATPO analogues.

Characterization of the Binding Site with GRID. The binding sites in the four ligand-binding core molecules (A−D) were analyzed with the GRID program[28] using water, methyl, and HPO_4^- probes (Figure 4a). The water probe pinpointed the experimental positions of most of the binding site waters. The binding site contained a 'dead spot' centered on the binding position of the isoxazole ring; this central region is too far from the protein to provide positive (enthalpic) contributions to binding according to GRID. Therefore, the isoxazole ring acts primarily as a spacer, and other scaffolds could potentially be used.

One difference noted between the largely similar binding sites of molecules A−D concerned the hydrogen phosphate probe, which picked up a broad region overlapping the experimentally determined positions of the phosphonate group of ATPO. However, the point of lowest energy was offset from the experimental position

by varying distances; in the case of ATPO:B, the most favored position was found ca. 1 Å away from the experimentally determined position of the phosphonate. Interestingly, the B-value for the phosphonate is highest in molecule B (data not shown). The flexibility of the ligand and the relatively broad zone between S654-T655 to which the phosphonate can bind according to GRID combine to give a more dynamic picture of the antagonist−receptor complex.

Mechanisms of Antagonism. Compared to the *apo* structure of S1S2J,[5] ATPO induces a domain closure ranging from 2.5 to 5.1° for the four molecules A−D. Approximately the same variance in domain closure is observed between the two protein molecules in the a.u. of DNQX (3.0 and 6.0°).[5] For comparison, the difference in domain closure between the two molecules in the *apo* structure is 3°.[5] Thus, while full agonists such as AMPA induce a domain closure of ca. 20°, the antagonists ATPO and DNQX stabilize an open conformation of the receptor, which is slightly closed compared to the *apo* structure.[5]

Even though ATPO and DNQX occupy different volumes of the binding site, both ligands fulfill the criteria for an antagonist, i.e. they both block further domain closure. Interestingly, this is achieved by a different set of interactions. ATPO stabilizes the open cleft via direct interactions between the phosphonate group and residues in domain 2. At the same time, the *tert*-butyl group is accommodated within the pocket formed by residues in domain 1 and domain 2. Thus, further domain closure is prevented by steric interference between the receptor and the *tert*-butyl group on one hand, and between the phosphonate moiety and domain 2 on the other. By contrast, the 6-nitro group of DNQX (at C8 in Figure 2b) prevents an interdomain interaction between Glu402 in domain 1 and Thr686 in domain 2 (Figure 3) and forms a long hydrogen bond (3.5 Å) to Thr686. In the closed agonist induced conformation of S1S2J, these two residues interact strongly.[5,19] Swanson et al.[29] reported that Asn721 in GluR6 (equivalent to Thr686 in GluR2) controls both AMPA sensitivity and domoate deactivation rates, pointing to the importance of this interdomain interaction for activation. Thus, ATPO and DNQX present two different and independent modes for preventing domain closure and stabilizing an open form of S1S2J.

All four molecules A−D form a 2-fold symmetric dimer with strictly symmetry-related molecules. The same dimer interface is observed in all known structures of GluR2-S1S2J in the open and closed forms.[5,19] However, rearrangement of the dimer interface has recently been shown to occur upon receptor desensitization.[10] Based on this repertoire of structures, a model has been proposed for activation and inactivation of iGluRs, in which iGluR tetramers are assembled from dimers-of-dimers and receptor activation is directly coupled to domain closure.[5,10] Moreover, inactivation by an antagonist is accomplished by stabilizing an open form of S1S2J, thereby preventing channel activation. The structure of S1S2J:ATPO is in accordance with this model.

Implications for Design of New Antagonists. Based on the crystallographic studies combined with the computational analysis, the binding site can be divided

into key regions (Figure 4b). The two sites I and II contain conserved residues crucial for binding the ligand. The counterpart for site I needs to be a hydrogen bond acceptor, whereas a hydrogen bond donor is preferred as counterpart to site II. Site III comprises a partly hydrophobic and partly polar cavity, conserved among AMPA receptors. The *tert*-butyl group is not optimized for this cavity, neither in terms of van der Waals contacts nor with respect to the possibility of specific polar interactions. Note also that Met708 borders the pocket and is known from agonist structures to be flexible, indicating the possibility of induced fit.[5,19] Site IV presents the crucial interdomain interaction between Glu402 and Thr686, which stabilizes the closed conformation of S1S2J in the agonist state.[5,19] Hindrance of this interaction stabilizes a resting, open conformation of the receptor.

Site V offers unused volume in the plane of the isoxazole ring, large enough to accommodate a substituted phenyl ring, for example. Interestingly, Tyr702 is located at the edge of this volume, nearly in plane with the isoxazole ring. It has been proposed that this tyrosine (corresponding to Tyr698 in GluR1) is the major determinant of selectivity between GluR1 and GluR3 for the agonist (*S*)-2-amino-3-(4-bromo-3-hydroxy-5-isoxazolyl)propionic acid (Br-HIBO).[30] In GluR3, this residue is a phenylalanine (Phe706). Consequently, this site shows great potential for the design of AMPA-subunit selective antagonists. As far as we are aware, no AMPA receptor antagonists have shown such subunit selectivity, in keeping with the fact that the antagonist lead structures DNQX and ATPO do not interact with site V.

Site VI offers the polar residues Ser654 and Thr655 from domain 2. Specific interactions with this site, in combination with occupation of site III, will inhibit domain closure, and antagonists may be designed on this basis. Interestingly, the antagonist [1,2,3,4-tetrahydro-7-morpholinyl-2,3-dioxo-6-(trifluoromethyl)quinoxalin-1-yl]methylphosphonate (ZK200775) may be considered as a hybrid of DNQX and ATPO, displaying high affinity binding to AMPA receptors (IC$_{50}$ of 0.12 μM).[31] Modeling studies suggest that the phosphonate group of ZK200775 is positioned at a similar position as the phosphonate group of ATPO and as the sulfate ion in the DNQX structure. Site VII presents Glu705, which forms an ion pair with the α-ammonium groups of all ligands in the reported S1S2J complex structures (except DNQX). Glu705 has also been implicated in the kinetics of domain closure.[5,32] The mouth of the cleft is depicted as site VIII. It is clear from the X-ray structures that ligands with a suitably positioned chain could thread in this direction out of the binding site. Such an approach could potentially be used to design high affinity and selective antagonists because the various subunits display different environments in this region.

Conclusion

The high-resolution X-ray structure of S1S2J:ATPO illustrates a new mode by which an open form of the AMPA receptor-binding site can be stabilized. By contrast with agonists, which induce substantial domain closure, the competitive antagonist ATPO induces minimal domain closure, thus supporting the hypothesis that antagonism of full length AMPA receptors is obtained by stabilizing an open cleft conformation of S1S2J (*apo*), as proposed by Armstrong et al.[5] Comparing S1S2J: ATPO with S1S2J:DNQX provides a more detailed description of the ligand-binding site and reveals key residues for antagonist recognition. The model derived on the basis of the results reported here may serve as a basis for the design of novel selective antagonists at AMPA receptors. Analysis of the two ligands indicates that the affinity of ATPO suffers from the entropic penalty imposed by flexibility. Antagonists of this type may be capable of achieving high selectivity, but are less likely to reach the potency of the highest affinity DNQX derivatives, due to the inherent cost of desolvating triionic species.

Experimental Section

Construct Design, Expression, Refolding, and Purification. The GluR2-S1S2 construct S1S2J was developed by Armstrong et al.[5] Protein expression, refolding, and purification were performed as previously described.[33]

Compound Synthesis and Activity Assay. The antagonist (*S*)-ATPO was synthesized and resolved as described and kindly provided by members of the Department of Medicinal Chemistry.[21,22] The [³H]AMPA K_D and the IC$_{50}$ values were measured for S1S2J as described.[18] Briefly, for the displacement experiments the protein sample (0.4 μg) was incubated with 20 nM [³H]AMPA (10.6 Ci/mmol) for 3 h on ice in AMPA binding buffer (30 mM TRIS-HCl pH 7.2, 100 mM KSCN, 2.5 mM CaCl$_2$, 10% glycerol) in a 0.5 mL volume. The incubations were performed in the presence of increasing concentrations of unlabeled ATPO (0.2 nM−4.0 mM). For the saturation-binding assay, the protein was incubated with 1.5−200 nM [³H]AMPA (10.6 Ci/mmol). Ligand binding experiments were carried out in duplicate.

Crystallization of S1S2J:ATPO, Data Collection, and Structure Refinement. A 10 mg/mL preparation (as determined by 1.0 OD$_{280}$ $\cong$ 0.8 mg/mL) of S1S2J in 10 mM HEPES pH 7.0, 20 mM NaCl, and 1 mM EDTA was used for crystallization. Final ligand concentration was 10 mM (*S*)-ATPO. Crystals were grown by the hanging drop vapor diffusion method at 6 °C by mixing the protein with an equal volume of precipitant solution. ATPO cocrystals were grown in 20% PEG 3350, 0.2 M ammonium sulfate, and 0.1 M sodium acetate pH 5.2. The reservoir volume was 0.5 mL. Prior to data collection, crystals were briefly soaked in the crystallization buffer containing ATPO and 15% glycerol before being flash-cooled in liquid nitrogen. Synchrotron data for S1S2J:ATPO were collected on the ESRF beamline ID14-1, Grenoble, France, using a MAR 165 mm CCD detector. The data were collected at 110 K. Data processing was performed using Denzo, Scalepack,[34] and the CCP4 suite of programs.[35] For further details see Table 1.

With four molecules in the a.u. of the S1S2J:ATPO unit cell, the Matthews coefficient V_m is 2.4 Å^3 Da^{-1}. A native Patterson was calculated using CCP4[35] in order to search for molecules related by pseudo translation symmetry. Two significant peaks, except for the origin peak, were found at 0, 0, 1/4 and 0, 0, 1/2, corresponding to 27.0% and 12.4% of origin peak, respectively, indicating that the molecules in the a.u. are related by simple translation symmetry of 1/4. The structure of S1S2J:ATPO was solved by molecular replacement (MR) using AMoRe[36] with the structure of S1S2J:DNQX (PDB id code 1FTL, molecule A, without water molecules and ligand)[5] as a search model. The best solution to the rotation and translation search was fixed and used to search for the translation of the second molecule. Subsequently, the translation solutions of molecule three and four were found by fixing two and three molecules, respectively. The final solution for the four molecules was improved after 30 cycles of rigid body refinement using AMoRe (correlation coefficient = 72.0, R_{factor} = 38.2).

The initial model was partly built and refined with the program ARP/wARP version 5.1[37] using the phases from the MR solution. The *warpNtrace* and *solvent* procedures within ARP/wARP automatically built 89% of the residues and the majority of the water molecule architecture, respectively. At this stage, ligands and ions could be unambiguously placed into the $F_o - F_c$ map. The structure was completed after three cycles of manual rebuilding in the program O[38] and refinements using CNS version 1.0.[39] The structure was refined using the data from the highest to the lowest resolution bin during the whole refinement procedure. The refinement protocol consisted of maximum-likelihood refinements and individual B-factor refinements. Coordinates for (*S*)-ATPO were retrieved from the inverted X-ray structure of *(R)-*ATPO.[21] Topology and parameter files for ATPO were generated by the HIC-Up server[40] and included into the crystallographic refinement and program O. The final electron density map was of excellent quality (Figure 1b). The structure has been deposited at the Protein Data Bank (id code 1N0T).

Solvation Calculations. ATPO and DNQX were optimized with ab initio density functional theory, using the PB-SCRF continuum model in Jaguar 4.1[41] at the B3LYP/6-311+G(d,p) level. The solvation energy of ATPO is difficult to determine by continuum solvation models because the molecule is flexible, charged, and capable of intra- as well as intermolecular hydrogen bonding. Optimization was carried out starting from both the global minimum derived from the Monte Carlo search (MMFFs) and also with dihedral angles constrained to those found in S1S2J:ATPO.[42] ($\Delta G_{solv} \approx -88$ kcal/mol for intramolecularly hydrogen bonded conformation of ATPO (optimized starting from the MMFFs/GB-SA global energy minimum conformation). For the constrained bioactive conformation, $\Delta G_{solv} \approx -134$ kcal/mol, according to DFT/PB-SCRF)

Monte Carlo Analysis. ATPO was subjected to 10000 Monte Carlo steps, as the free tri-ionized ligand. The analysis was repeated with either butyrate (mimicking Glu705) or three explicit water molecules included, with loose flat-bottomed constraints to keep the system closed. The analysis was also performed with the four major dihedral angles (C1−C, C−C6, C5−O3, O3−C4, see Figure 2a) constrained to those found in S1S2J:ATPO. The force field used was MMFFs with GB-SA continuum treatment of water in Macromodel 7.2.[42]

GRID Mapping of the Binding Sites. All four binding sites within the a.u. were analyzed in the absence of the ligand or other HETATM records using GRID 18[28] at a grid of 1/3 Å. Three probes were used: water, methyl, and HPO_4^- probes; otherwise default settings were used. The binding site grid maps were visualized in InsightII.[43]

References

(1) Dingledine, R.; Borges, K.; Bowie, D.; Traynelis, S. F. The glutamate receptor ion channels. *Pharmacol. Rev.* **1999**, *51*, 7−61.

(2) Parsons, C. G.; Danysz, W.; Quack, G. Glutamate in CNS disorders as a target for drug development: An update. *Drug News Perspect.* **1998**, *11*, 523−569.

(3) Hollmann, M.; Heinemann, S. Cloned glutamate receptors. *Annu. Rev. Neurosci.* **1994**, *17*, 31−108.

(4) Borges, K.; Dingledine, R. AMPA receptors: Molecular and functional diversity. *Prog. Brain Res.* **1998**, *116*, 153−170.

(5) Armstrong, N.; Gouaux, E. Mechanisms for activation and antagonism of an AMPA-sensitive glutamate receptor: Crystal structures of the GluR2 ligand binding core. *Neuron* **2000**, *28*, 165−181.

(6) Robert, A.; Irizarry, S. N.; Hughes, T. E.; Howe, J. R. Subunit interactions and AMPA receptor desensitization. *J. Neurosci.* **2001**, *21*, 5574−5586.

(7) Mansour, M.; Nagarajan, N.; Nehring, R. B.; Clements, J. D.; Rosenmund, C. Heteromeric AMPA receptors assemble with a preferred subunit stoichiometry and spatial arrangement. *Neuron* **2001**, *32*, 841−853.

(8) Mayer, M. L.; Olson, R.; Gouaux, E. Mechanisms for ligand binding to GluR0 ion channels: Crystal structures of the glutamate and serine complexes and a closed apo state. *J. Mol. Biol.* **2001**, *311*, 815−836.

(9) Ayolan, G.; Stern-Bach, Y. Functional assembly of AMPA and kainate receptors is mediated by several discrete protein−protein interactions. *Neuron* **2001**, *31*, 103−113.

(10) Sun, Y.; Olson, R.; Horning, M.; Armstrong, N.; Mayer, M.; Gouaux, E. Mechanism of glutamate receptor desensitization. *Nature* **2002**, *417*, 245−253.

(11) Sommer, B.; Keinänen, K.; Verdoorn, T. A.; Wisden, W.; Burnashev, N.; Herb, A.; Köhler, M.; Takagi, T.; Sakmann, B.; Seeburg, P. H. Flip and Flop: A cell-specific functional switch in glutamate-operated channels of the CNS. *Science* **1990**, *249*, 1580−1585.

(12) Seeburg, P. H. The role of RNA editing in controlling glutamate receptor channel properties. *J. Neurosci.* **1996**, *66*, 1−5.

(13) Seeburg, P. H. The TINS/TIPS Lecture. The molecular biology of mammalian glutamate receptor channels. *Trends Neurosci.* **1993**, *16*, 359−365.

(14) Stern-Bach, Y.; Bettler, B.; Hartely, M.; Sheppard, P.; O'Hara, P. J.; Heinemann, S. F. Agonist selectivity of glutamate receptors is specified by two domains structurally related to the bacterial amino acid-binding proteins. *Neuron* **1994**, *13*, 1345−1357.

(15) Kuusinen, A.; Arvola, M.; Keinänen, K. Molecular dissection of the agonist binding site of an AMPA receptor. *EMBO J.* **1995**, *14*, 6327−6332.

(16) Wo, Z. G.; Oswald, R. E. Transmembrane topology of two kainate receptor subunits revealed by N-glycosylation. *Proc. Natl. Acad. Sci. U. S. A.* **1994**, *91*, 7154−7158.

(17) Amstrong, N.; Sun, Y.; Chen, G. Q.; Gouaux, E. Structure of a glutamate-receptor ligand-binding core in complex with kainate. *Nature* **1998**, *395*, 913−917.

(18) Chen, G. Q.; Gouaux, E. Overexpression of a glutamate receptor (GluR2) ligand binding domain in Escherichia coli: Application of a novel protein folding screen. *Proc. Natl. Acad. Sci. U. S. A.* **1997**, *94*, 13431−13436.

(19) Hogner, A.; Kastrup, J. S.; Jin, R.; Liljefors, T.; Mayer, M. L.; Egebjerg, J.; Larsen, I. K.; Gouaux, E. Structural basis for AMPA receptor activation and ligand selectivity: Crystal structures of five agonist complexes with the GluR2 ligand binding core. *J. Mol. Biol.* **2002**, *322*, 93−109.

(20) Bräuner-Osborne, H.; Egebjerg, J.; Nielsen, E. Ø.; Madsen, U.; Krogsgaard-Larsen, P. Ligands for glutamate receptors: Design and therapeutic prospects. *J. Med. Chem.* **2000**, *43*, 2609−2645.

(21) Madsen, U.; Bang-Andersen, B.; Brehm, L.; Christensen, I. T.; Ebert, B.; Kristoffersen, I. T. S.; Lang, Y.; Krogsgaard-Larsen, P. Synthesis and pharmacology of highly selective carboxy and phosphono isoxazole amino acid AMPA receptor antagonists. *J. Med. Chem.* **1996**, *39*, 1682−1691.

(22) Møller, E. H.; Egebjerg, J.; Brehm, L.; Stensbøl, T. B.; Johansen, T. N.; Madsen, U.; Krogsgaard-Larsen, P. Resolution, absolute stereochemistry, and enantiopharmacology of the GluR1-4 and GluR5 antagonist 2-amino-3-[5-*tert*-butyl-3-(phosphonomethoxy)-4-isoxazolyl]propionic acid. *Chirality* **1999**, *11*, 752−759.

(23) Keinänen, K.; Wisden, W.; Sommer, B.; Werner, P.; Herb, A.; Verdoorn, T. A.; Sakmann, B.; Seeburg, P. H. A family of AMPA-selective glutamate receptors. *Science* **1990,** *249*, 556−560.

(24) Rodrigues, M. A.; Brochsztain, S.; Barros, T. C.; Baptista, M. S.; Politi, M. J. pH-Dependent excited-state properties of N,N-9-di(2-phosphonoethyl)-1,4,5,8-naphthalenediimide. *Photochem. Photobiol.* **1999**, *70*, 35−39.

(25) Madden, D. R.; Thiran, S.; Zimmermann, H.; Romm, J.; Jayaraman, V. Stereochemistry of quinoxaline antagonist binding to a glutamate receptor investigated by Fourier transform infrared spectroscopy. *J. Biol. Chem.* **2001**, *276*, 37821−37826.

(26) Stensbøl, T. B.; Madsen, U.; Krogsgaard-Larsen, P. The AMPA receptor binding site: Focus on agonists and competitive antagonists. *Curr. Pharm. Des.* **2002**, *8*, 857−872.

(27) Doig, A. J.; Sternberg, M. J. Side-chain conformational entropy in protein folding. *Protein Sci.* **1995**, *11*, 2247−2251.

(28) Goodford, P. J. A computational procedure for determining energetically favorable binding sites on biologically important macromolecules. *J. Med. Chem.* **1985**, *28*, 849−857.

(29) Swanson, G. T.; Gereau, R. W. T.; Green, T.; Heinemann, S. F. Identification of amino acid residues that control functional behavior in GluR5 and GluR6 kainate receptors. *Neuron* **1997**, *19*, 913−926.

(30) Banke, T. G.; Greenwood, J. R.; Christensen, J. K.; Liljefors, T.; Traynelis, S. F.; Schousboe, A.; Pickering, D. S. Identification of amino acid residues in GluR1 responsible for ligand binding and desensitization. *J. Neurosci.* **2001**, *21*, 3052−3062.

(31) Turski, L.; Huth A.; Sheardown, M.; McDonald, F.; Neuhaus, R.; Schneider H. H.; Dirnagl U.; Wiegand, F.; Jacobsen, P.; Ottow E. ZK200775: A phosphonate quinoxalinedione AMPA antagonist for neuroprotection in stroke and trauma. *Proc. Natl. Acad. Sci. U. S. A.* **1998**, *95*, 10960−10965.

(32) Abele, R.; Keinänen, K.; Madden, D. R. Agonist-induced isomerization in a glutamate receptor ligand-binding domain. A kinetic and mutagenetic analysis. *J. Biol. Chem.* **2000**, *275*, 21355−21363.

(33) Chen, G. Q.; Sun, Y.; Jin, R.; Gouaux, E. Probing the ligand binding domain of the GluR2 receptor by proteolysis and deletion mutagenesis defines domain boundaries and yields a crystallizable construct. *Protein Sci.* **1998**, *7*, 2623−2630.

(34) Otwinowski, Z.; Minor, W. Processing of X-ray diffraction data collected in oscillation mode. *Methods Enzymol.* **1997**, *276*, 307−326.

(35) Collaborative Computational Project, Number 4. The CCP4 Suite: Programs for Protein Crystallography. *Acta Crystallogr.* **1994**, *D50*, 760−763.

(36) Navaza, J. *AMoRe*: An automated package for molecular replacement. *Acta Crystallogr.* **1994**, *A50*, 157−163.

(37) Perrakis, A.; Morris, R.; Lamzin, V. S. Automated protein model building combined with iterative structure refinement. *Nat. Struct. Biol.* **1999**, *6*, 458−463.

(38) Jones, T. A.; Zou, J. Y.; Cowan, S. W.; Kjeldgaard, M. Improved methods for binding protein models in electron density maps and the location of errors in these models. *Acta Crysallogr.* **1991**, *A47*, 110−119.

(39) Brünger, A. T.; Adams, P. D.; Clore, G. M.; DeLano, W. L.; Gros, P.; Grosse-Kunstleve, R. W.; Jiang, J. S.; Kuszewski, J.; Nilges, M.; Pannu, N. S.; Read, R. J.; Rice, L. M.; Simonson, T.; Warren, G. L. Crystallography & NMR system: A new software suite for macromolecular structure determination. *Acta Crystallogr.* **1998**, *D54*, 905−921.

(40) Kleywegt, G. J.; Jones, T. A. Databases in protein crystallography. *Acta Crystallogr.* **1998**, *D54*, 1119−1131.

(41) Jaguar 4.1, Schrödinger, Inc., 1500 S.W. First Avenue, Suite 1180 Portland, OR 97201, 2001.

(42) Macromodel 7.2, Schrödinger Inc., 1500 S.W. First Avenue, Suite 1180 Portland, OR 97201, 2001.

(43) Insight II, Accelrys Inc., 200 Wheeler Road South Tower, Burlington, MA, 2000.

(44) Kleywegt, G. J.; Jones, T. A. Phi/Psi-chology: Ramachandran revisited. *Structure* **1996**, *4*, 1395−1400.

(45) Wallace, A. C.; Laskowski, R. A.; Thornton, J. M. LIGPLOT: A program to generate schematic diagrams of protein−ligand interactions. *Protein Eng.* **1995**, *8*, 127−134.

(46) Kraulis, P. J. Molscript: A program to produce both detailed and schematic plots of protein structures. *J. Appl. Crystallogr.* **1991**, *24*, 946−950.

(47) Merritt, E. A.; Murphy, M. E. P. Raster3D version 2.0. A program for photorealistic molecular graphics. *Acta Crystallogr.* **1994**, *D50*, 869−873.